ISSN 0021-3640, JETP Letters, 2011, Vol. 94, No. 8, pp. 635–641. © Pleiades Publishing, Inc., 2011.
Original Russian Text © S.V. Grigoriev, N.A. Grigoryeva, K.S. Napol'skii, A.P. Chumakov, A.A. Eliseev, I.V. Roslyakov, H. Eckerlebe, A.V. Syromyatnikov, 2011, published in Pis'ma v Zhurnal Eksperimental'noi i Teoreticheskoi Fiziki, 2011, Vol. 94, No. 8, pp. 678–684.

Arrays of Interacting Ferromagnetic Nanofilaments: Small-Angle Neutron Diffraction Study

S. V. Grigoriev[a], N. A. Grigoryeva[b, *], K. S. Napol'skii[c], A. P. Chumakov[a], A. A. Eliseev[c], I. V. Roslyakov[c], H. Eckerlebe[d], and A. V. Syromyatnikov[a, b]

[a] *Konstantinov Petersburg Nuclear Physics Institute, Russian Academy of Sciences, Gatchina, 188301 Russia*
[b] *St. Petersburg State University, St. Petersburg, 199034 Russia*
* *e-mail: natali@lns.pnpi.spb.ru*
[c] *Moscow State University, Moscow, 119991 Russia*
[d] *Helmholtz-Zentrum Geesthacht, Geesthacht, 21502 Germany*

Received September 8, 2011

Magnetic properties of spatially ordered arrays of interacting nanofilaments have been studied by means of small-angle diffraction of polarized neutrons. Several diffraction maxima or rings that correspond to the scattering of the highly ordered structure of pores/filaments with hexagonal packing have been observed in neutron scattering intensity maps. The interference (nuclear-magnetic) and pure magnetic contributions to the scattering have been analyzed during the magnetic reversal of the nanofilament array in a field applied perpendicular to the nanofilament axis. The average magnetization and the interference contribution proportional to it increase with the field and are saturated at $H = H_S$. The magnetic reversal process occurs almost without hysteresis. The intensity of the magnetic contribution has hysteresis behavior in the magnetic reversal process for both the positive and negative fields that form the field dependence of the intensity in a butterfly shape. It has been shown that this dependence is due to the magnetostatic interaction between the filaments in the field range of $H \le H_S$. A theory for describing the magnetic properties of the arrays of interacting ferromagnetic nanofilaments in the magnetic field has been proposed.

DOI: 10.1134/S0021364011200057

1. INTRODUCTION

A study of the magnetic properties of the arrays of interacting ferromagnetic nanofilaments, the transverse dimensions of which are much less than their length, is of doubtless interest with respect to the concept of miniaturization of the element base of electronics. Usually an individual nanofilament is considered to be a single working element, the effect of the other array elements on which is considered to be negligibly small (see, e.g., [1] and references therein), since nanofilaments interact with each other by means of the weak dipole interaction. This ignoring the interaction is quite correct when the density of nanofilaments in the sample f (the ratio of the volume of all nanofilaments to the total volume of the sample) is low. For example, the interaction for nickel nanofilaments can be neglected if the order of magnitude of f is smaller than 0.01. For an array of nanofilaments ordered into a square lattice, this corresponds to the ratio of the filament radius to the distance between the centers $R/a = 0.05$. However, at denser packing ($R/a \gg 0.05$), it is impossible to ignore the interaction between nanofilaments, since it strongly changed the properties of the array on the whole. In particular, the long-range magnetic order may arise in the spatially ordered array of nanofilaments as a result of their magnetic interaction.

The spatial ordering is determined by a template, based on which an array is created. The ordering degree of both the template and the array of nanofilaments can be studied by the small-angle X-ray diffraction method [2]. In turn, a natural instrument for measuring the magnetic ordering is the small-angle neutron diffraction on the array of nanofilaments, since the magnetic component of the neutron diffraction or the integral intensity of the magnetic reflections is proportional to the square of the number of the coherently scattering filaments N^2. Thus, the change in the magnetic order in the array of nanofilaments can be determined directly from the change in the intensity of the magnetic component of Bragg reflections.

In this work, the magnetic properties of the spatially ordered arrays of magnetic nanofilaments are studied by the method of the small-angle diffraction of polarized neutrons. The magnetic reversal of the arrays of nanofilaments in the field applied perpendicular to the filament axis is studied. It is established that the magnetic contribution to the scattering intensity has a hysteresis behavior in the magnetic reversal process for both the positive and negative fields forming the field

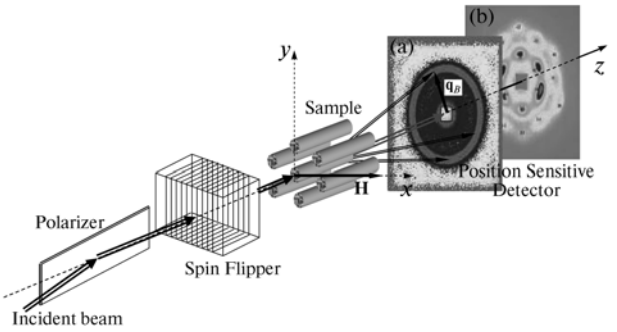

Fig. 1. Scheme of the experiment on small-angle diffraction of polarized neutrons on two-dimensional arrays of nanofilaments. Diffraction patterns correspond to the small-angle scattering on the (a) Fe/SiO_2 powder sample and (b) Ni/Al_2O_3 film.

dependence of the intensity in the butterfly wings shape. In this work, special attention was focused on the elaboration of a theory that describes the magnetic properties of the arrays of interacting ferromagnetic nanofilaments in the magnetic field.

2. EXPERIMENT

2.1. Synthesis of Samples

We investigated (i) a powder sample made of mesoporous silicon dioxide particles with iron nanofilaments introduced into the pores and (ii) a quasi-single crystal, i.e., an array of nickel nanofilaments formed on the basis of the porous aluminum oxide films.

A magnetic powder nanocomposite Fe/SiO_2 is an array of nanofilaments obtained on the basis of mesoporous silicon dioxide by introducing a nonpolar metal complex (carbonyl $Fe(CO)_5$) into the hydrophobic part of the composite (pore) by impregnation with the subsequent decomposition under the action of the ultraviolet radiation and thermal crystallization. This technology allows one to obtain arrays of filament-like particles with lengths L on the order of 1–2 μm, diameters $2R$ of about 2 nm, and a on the order of 4 nm [3].

Al_2O_3 films 60 μm thick with a highly ordered hexagonal structure of pores ($a = 105$ nm) were used as a template for the synthesizing filament-like nanoparticles [4]. The controlled growth of Ni nanoparticles in a porous Al_2O_3 matrix was performed by the electrochemical deposition method in a three- electrode cell in the potentiostatic mode. The duration of the Ni electrodeposition was 24 h, which, according to the scanning electron microscopy data, corresponded to the formation of the filament-like nanoparticles with the length $L = 20$ μm. The diameter of the particles was $2R = 40$ nm [5].

2.2. Small-Angle Scattering of the Polarized Neutrons on the Ordered Magnetic Nanostructures

The neutron scattering cross section can be represented as a sum of three terms $\left|f_{\mathbf{q}}^2\right| = \Sigma_n + \Sigma_m + \Sigma_i$, where Σ_n and Σ_m are the nuclear and magnetic scattering cross sections, respectively, which do not depend on the neutron polarization $\mathbf{P}$, and Σ_i describes the nuclear-magnetic interference and is proportional to $\mathbf{P}$. The terms of the scattering cross section on the studied arrays of the magnetic nanofilaments can be written as [6]

$$\Sigma_n = A^2\left|\mathcal{S}(q)F(\mathbf{q})\right|^2, \quad (1)$$

$$\Sigma_m = B^2\left|\mathcal{S}(q)F(\mathbf{q})\right|^2, \quad (2)$$

$$\Sigma_i = 2AB\frac{(\mathbf{PM})}{M}\left|\mathcal{S}(q)F(\mathbf{q})\right|^2, \quad (3)$$

$$B = \frac{\pi L\mu_n m}{\hbar^2 k}\sqrt{M_z^2 + (1-N_\perp)^2 M_x^2}, \qquad A = kL(n_m - n_p)/2, \quad (4)$$

where $N_\perp = 1/2$ is the demagnetization factor in the direction perpendicular to the nanofilament, $M_{x,z}$ are the components of the magnetization of the total sample (the coordinate system is shown in Fig. 1), $\mathcal{S}(q) = 2kR^2J_s(qR)/(qR)$ is the form factor, $J_s(x)$ in the s-order Bessel function of the first kind, and $F(\mathbf{q}) = \sum_n \exp(-i\mathbf{q}\boldsymbol{\rho}_n)$ is the structural factor (the summation is performed over the position of the centers of nanofilaments given by the vectors $\boldsymbol{\rho}_n$). The structural factor $F(\mathbf{q})$ has maxima when $\mathbf{q}$ is equal to the reciprocal lattice vectors, i.e., $\mathbf{q}_{ht} = h\mathbf{a}_1 + t\mathbf{a}_2$, where h and t are integers, $\mathbf{a}_1 = (1, 0) \times 4\pi/(\sqrt{3}\,a)$ and $\mathbf{a}_2 = (1, \sqrt{3}) \times 2\pi/(\sqrt{3}\,a)$ are the unit vectors of the reciprocal lattice, and a is the distance between the centers of the neighboring filaments.

Note that, for the qualitative description of the neutron data, in Eqs. (2) and (3), we ignored the contribution of the magnetic field produced by the magnetic nanofilaments in the space between the pores. This is a rather correct approximation when the filaments are magnetized along their length [1], but it is not quite correct at a rather large transverse component of the magnetization. Taking into account the real geometry of the studied samples and that the field produced by the transversely magnetized long cylinder decreases with the distance r from the pore center as $1/r^2$ [7], one can state that Eqs. (2) and (3) can be used for the qualitative description.

The small-angle neutron scattering experiments were performed at the SANS-2 facility of the FRG-1 research reactor in Geesthacht (Germany). We used a polarized neutron beam with the initial polarization

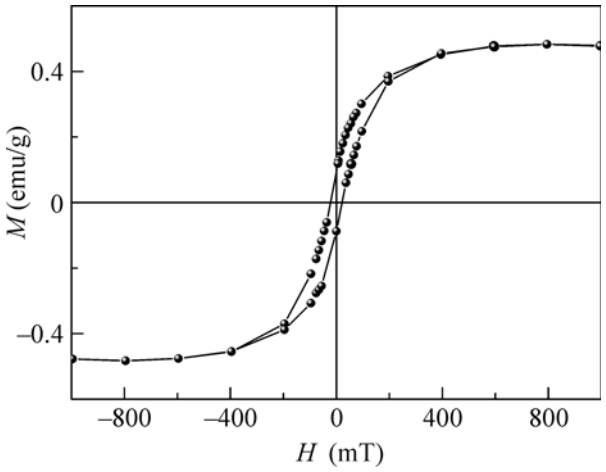

Fig. 2. Hysteresis curve of the magnetization of the Fe/SiO_2 sample at the temperature $T = 300$ K.

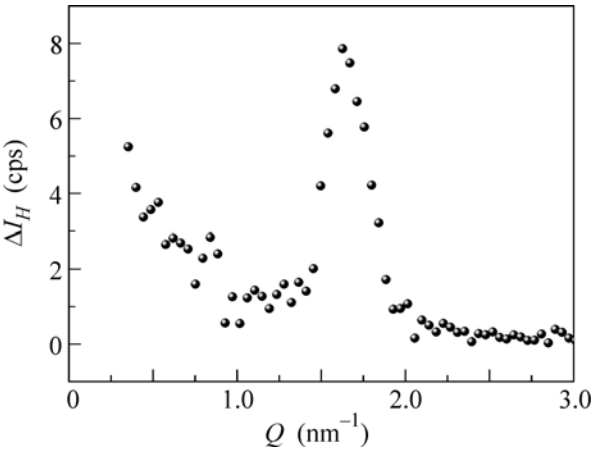

Fig. 3. Part of the neutron scattering intensity depending on the magnetic field for the Fe/SiO_2 sample in the magnetic field $H = 200$ mT (inverse course) at the temperature $T = 300$ K.

$P_0 = 0.95$, wavelength $\lambda = 0.58$ nm, ratio $\Delta\lambda/\lambda = 0.1$, and beam divergence of 1.5 mrad. The scattered neutrons were recorded on a two-coordinate position-sensitive detector with a resolution of 256 ×256 cells. The film of the Ni/Al_2O_3 sample with an area of about 0.5 cm^2 was oriented perpendicular to the neutron beam and was uniformly exposed over the total area. This geometry corresponds to the parallel orientation of the axis of the nanofilaments in the sample with respect to the incident neutron beam. In the case of the powder Fe/SiO_2 sample, the scattering pattern is a set of concentric rings, which are mainly due to scattering on the nanofilaments located parallel to the incident neutron beam (Fig. 1). This is because the coherent volume of neutrons scattered at small angles is effectively elongated along the beam, and the coherent volume of the system of nanofilaments is elongated along the filaments. When the filament axis coincides with the axis of the beam, the effectiveness of the scattering is increased by several times (see, e.g., [8]). The chosen geometry of the experiment allows one to observe a system of diffraction reflections from the ordered structure of the porous matrix and the superstructure of the magnetic nanofilaments in the small-angle scattering range.

The external magnetic field **H** was applied perpendicular to the axis of the incident neutron beam that corresponds to the geometry in which the field is perpendicular to the long axis of nanofilaments. In the experiments, the dependence of the scattering neutron intensity on the transmitted pulse at the neutron polarization directed parallel ($I(q, +P_0)$) and antiparallel ($I(q, -P_0)$) to the external magnetic field. Part of the neutron scattering cross section independent of the polarization (i.e., the sum of the nuclear and magnetic cross sections) was determined as the sum $I(q) = [I(q, +P_0) + I(q, -P_0)]/2$. The magnetic component of the total scattering cross section was estimated as the contribution $I_H(q) = I(q, H) - I(q, 0)$ depending on the magnetic field. The scattering depending on the neutron polarization, $\Delta I(q) = [I(q, +P_0) - I(q, -P_0)]/2$, is the interference contribution and it characterizes the extent of correlation between the nuclear and magnetic structures.

3. RESULTS OF MEASUREMENTS

Figure 2 shows the hysteresis curve of the magnetization of the Fe/SiO_2 powder sample in which the axis of the nanofilaments is randomly oriented with respect to the direction of the magnetic field. The magnetization demonstrates a slight hysteresis with the coercive force $H_c \sim 20$ mT and saturation in the field $H_S \sim 400$ mT. Small-angle diffraction on this sample is a ring (a system of rings) of the scattering intensity as is shown on the detector in Fig. 1a. The Q dependence of the magnetic component of the neutron scattering $\Delta I_H(Q)$ for the Fe/SiO_2 sample in the magnetic field $H = 300$ mT applied perpendicular to the beam is presented in Fig. 3. The position of the diffraction magnetic peak coincides with the maximum of the nuclear scattering cross section at the momentum transfer $Q = 1.65$ nm^{-1}. The distance a between the filaments calculated under the assumption of the hexagonal packing of the filaments is 4.4 nm. The dependence $\Delta I_H(Q)$ is the difference of the magnetic cross sections of the sample in the two different states, namely, the state close to the saturation magnetization (in the field $H = 200$ mT) and the completely demagnetized state at $H = 0$.

The change in the magnetic component of the Bragg reflection I_H at $Q = 1.65$ nm^{-1} for the Fe/SiO_2 sample during the magnetic reversal of the sample is given in Fig. 4. In the magnetization process, the

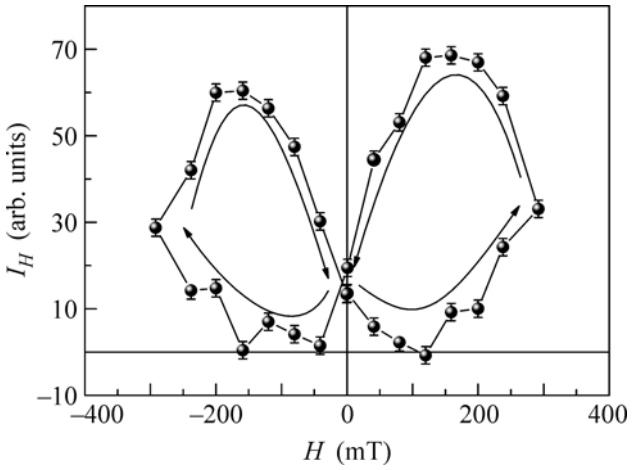

Fig. 4. Magnetic field dependence of the magnetic part of the intensity I_H of the Bragg reflection at $Q = 1.65$ cm^{-1} for the Fe/SiO_2 sample at $T = 300$ K.

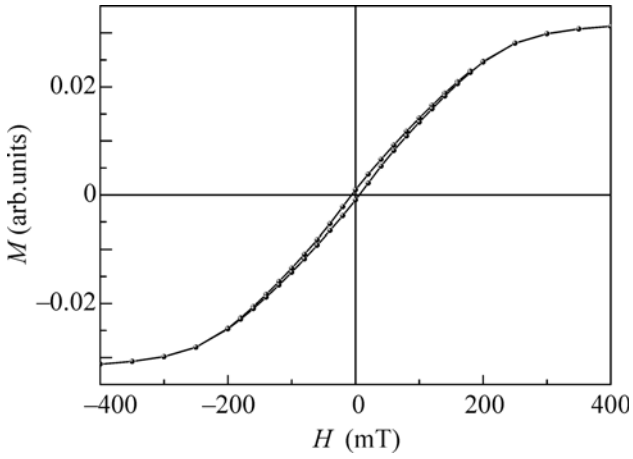

Fig. 5. Hysteresis curve of the magnetization of the Ni/Al_2O_3 sample at the temperature $T = 300$ K in the field perpendicular to the nanofilament axis.

intensity of the reflection at $|H| < 100$ mT first decreases somewhat with an increase in the external magnetic field, then increases up to the reversal point at $H = 300$ mT. When the external magnetic field decreases, the intensity of the reflection at $|H| > 100$ mT first increases sharply, then decreases to the initial value as the field approaches zero.

Note that this behavior of the magnetic reflection intensity during the magnetic reversal process is general and is also observed at low temperatures down to $T = 10$ K. In all cases, the interference contribution $\Delta I(q)$ to the Bragg reflection for the powder Fe/SiO_2 sample was statistically unresolved. However, taking into account that the intensity of the interference contribution is proportional to the projection of the magnetization onto the direction of the external magnetic field, it can be supposed that the magnetization hysteresis curve in Fig. 2 gives a complete idea about the behavior of the interference contribution to the scattering as well.

To emphasize the typical nature of the phenomenon, let us present data about the magnetic reversal process in the array of the magnetic nickel nanofilaments in the porous Al_2O_3 matrix in the field tansverse to the filament axis. Figure 5 shows the magnetization hysteresis curve of the Ni/Al_2O_3 quasi-single crystal for the magnetic field perpendicular to the nanofilament axis. The magnetization demonstrates a slight hysteresis with the coercive force $H_c \sim 10$ mT and with the saturation in the field $H_S \sim 350$ mT typical for nickel.

It was shown in [6] and Fig. 1b that several diffraction maxima are clearly visible at the small-angle diffraction of polarized neutrons on the Ni/Al_2O_3 sample, which indicates the highly ordered structure of the studied nanocomposite. The observed diffraction maxima were indicated in the hexagonal system with the lattice parameter $a_0 = 106 \pm 2$ nm. The intensity $I_H(Q)$ of the Bragg peaks depending on the magnetic field and the interference nuclear-magnetic contribu-

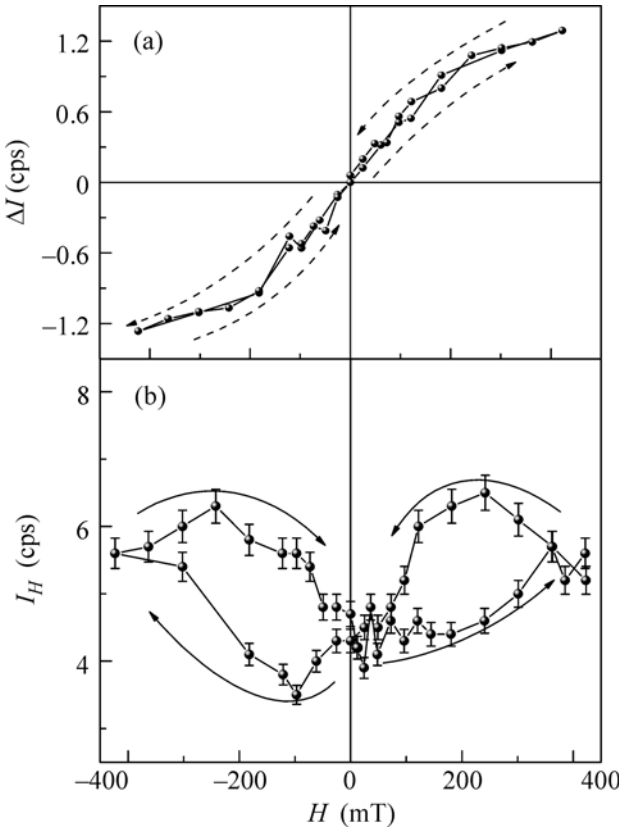

Fig. 6. Field dependence of the intensities of the (a) interference contribution $\Delta I(Q_{10})$ and (b) magnetic coherent contribution $I_H(Q_{10})$.

tion $\Delta I(Q)$ to these peaks were separated. The field dependences of the intensities $\Delta I(Q)$ and $I_H(Q)$ of the most intense magnetic reflection at $\mathbf{Q} = \mathbf{Q}_{10}$ are shown in Fig. 6. The interference contribution to the reflection $\Delta I(Q_{10})$ is proportional to the average magnetization of the individual nanofilament in the projection onto the magnetic field direction (see Eq. (3)). The intensity of the interference contribution has no hysteresis (Fig. 6a). This behavior agrees rather well with the SQUID magnetometry data (Fig. 5). The intensity of the magnetic component $I_H(Q)$ is described by the hysteresis dependences for both positive and negative fields with the increase and the subsequent decrease in the magnetic field.

Thus, the field dependence of the magnetic contribution to the neutron scattering for different samples of the arrays of the magnetic nanofilaments is characteristic (butterfly shape; Figs. 4 and 6b) with hysteresis for the positive and negative fields at $0 < H < H_S$. The lower branch of the hysteresis, when the slight change in the intensity of the magnetic scattering is observed, corresponds to the increase in the field in the absolute value, and the lower branch to the decrease in the field, when the sharp increase in the intensity and its subsequent gradual decrease when the magnetic field approaches zero are observed.

4. INTERPRETATION

4.1. Isolated Nanofilament in the Magnetic Field

To interpret results of the neutron studies, first consider the behavior of an isolated nanofilament in the magnetic field. The free energy of the unit volume of a homogeneously magnetized nanofilament placed in the homogeneous external magnetic field H has the simple form [1]

$$\mathcal{F} = -\pi M_s^2 \cos^2\theta - M_s H \cos(\theta - \theta_h), \qquad (5)$$

where θ and θ_h are the polar angles of the magnetization and field, respectively, counted from the filament axis and M_s is the magnetic moment of the unit volume (Fig. 7). The first term in Eq. (5) describes the anisotropy of the shape, due to which the filament axis is the easy magnetization direction and the magnetic moment of the filament is not parallel to the field, i.e., $\theta_h \neq 0, \pi$. If the angle between the field and the initial magnetization direction is acute, the magnetization process occurs smoothly; the angle θ continuously increases from 0 and reaches θ_h in the limit of the infinitely high field. If $\theta_h = \pi/2$, then $\theta = \theta_h$ at $H = H_S = 2\pi M_s$. In the case of the obtuse angle, the magnetization component on the filament axis changes sign stepwise (the filament experiences the magnetic reversal) at a certain field value $H_f(\theta_h)$ (Fig. 7).

At present, there is no theory that provides an analytical expression for $H_f(\theta_h)$ that would quantitatively describe all experimental data [1]. Let us consider in short the main approaches to the calculations of $H_f(\theta_h)$. In the first of them (coherent model [9]), it is assumed that, in the magnetic reversal process, the filament remains homogeneously magnetized. In this case, the free energy given by Eq. (5) at low H has two minima (Fig. 7). The energies of these minima are the same only when the field is applied perpendicular to the filament axis. Otherwise, one of them describes a metastable state, which disappears with the increase in the field up to the $H_f(\theta_h)$ value. After simple calculations with the use of Eq. (5), it is possible to obtain $H_f^{\mathrm{coh}}(\theta_h) = (\cos^{2/3}\theta_h + \sin^{2/3}\theta_h)^{-3/2}$ [1]. However, the experimental magnetic reversal data on rather thick nanofilaments are qualitatively correctly described by another theory (curling model [9]), which assumes that the magnetic reversal occurs via the state with the inhomogeneous magnetization of the nanofilament. The behavior $H_f^{\mathrm{cur}}(\theta_h)$ in this model at $\theta_h > \pi/4$ resembles the behavior $H_f^{\mathrm{coh}}(\theta_h)$, and at $\theta_h < \pi/4$ $H_f^{\mathrm{cur}}(\theta_h)$ is approximately constant.

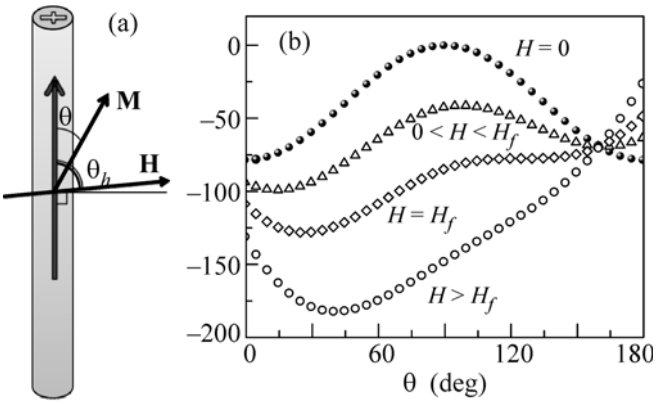

Fig. 7. (a) Orientation of the applied field and magnetization for the isolated nanofilament. (b) Free energy $\mathcal{F}$ versus the θ angle at the magnetic fields applied at the angle $\theta_h = 70°$.

4.2. Array of Interacting Nanofilaments in the Magnetic Field

Let us consider an array of nanofilaments in the magnetic field perpendicular to the axes of filaments. It is important to take into account the following circumstance. If the field is lower than the saturation field $H_S = 2\pi M_s$, the filaments have a nonzero magnetization component along their axis. If the number of the filaments N_+ with the positive transverse component is larger than the number of the filaments with the negative transverse component $N_- = N - N_+$, where N

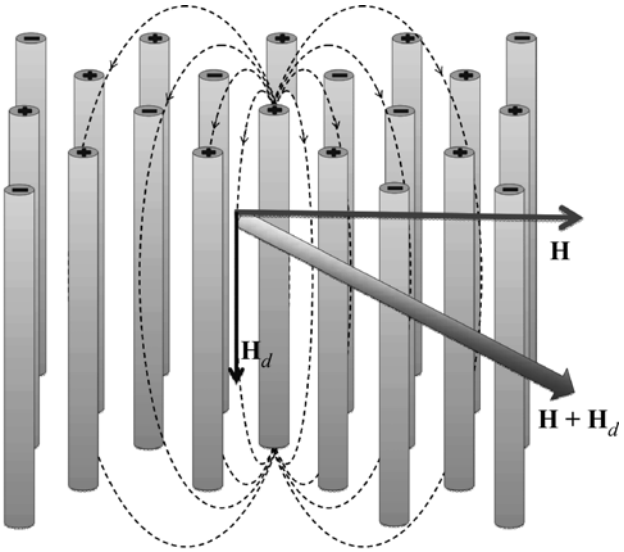

Fig. 8. Schematic distribution of the magnetic fields $\mathbf{H} + \mathbf{H}_d$ in the array of the magnetic nanofilaments.

is the number of all filaments, the following demagnetizing field appears:

$$\mathbf{H}_d = -4\pi f\left(\frac{N_+}{N}\mathcal{M}_z^+ - \frac{N_-}{N}\mathcal{M}_z^-\right)\mathbf{n}_z, \qquad (6)$$

where $\mathbf{n}_z$ is the unit vector along the z axis parallel to the axes of the filaments and $\mathcal{M}_z^\pm$ are the corresponding projections of the magnetization of the unit volume of the filaments. This field, as well as the anisotropy of the shape in Eq. (5), is due to the magnetic dipole interaction. The field $\mathbf{H}_d$ tends to equalize the N_+ and N_- numbers, which makes the state of the majority of filaments energy-unfavorable (see Fig. 8).

Note that, in this case, the appearance of the demagnetizing field is the only effect related to the interaction between the filaments. In the considered case, the effect of the nearest filaments on each other is negligibly small (the effective field created by the filament magnetized parallel to its axis in the location of the neighboring filament is less than 1 Oe). At the same time, this field changes very slightly at distances r from the filament that are less than length L; it decreases as $1/r^3$ only at $r \gg L$ [1]. Since the distance between the nearest nanofilaments is several orders of magnitude shorter than their length, the given filament is affected by the large number ($\sim(L/a)^2$) of its neighbors located within the radius L from it. Thus, the effect of the total array of filaments on a particular filament is reduced to the appearance of an (average) magnetic field (the same for all nanofilaments), which is obviously equal to the demagnetization field. As a result, when studying the magnetic reversal processes in the array of filaments, it is sufficient to analyze the behavior of only two filaments with positive and negative projections of magnetization onto their axis in the field $\mathbf{H} + \mathbf{H}_d$ (Fig. 8).

Let us start with the case of a very strong field that aligns the magnetizations of all filaments parallel to their axes. According to Eq. (5), the component of the magnetization of the filaments parallel to their axes arises at $H < H_S$. In this case, the sign of this projection for each separate filament may be both positive and negative because the energy Eq. (5) has two equivalent minima. If the magnetic dipole interaction is taken into account, it follows from the simple condition of the minimum of the bulk magnetic energy [7] that the energy-favorable configurations are those in which the numbers of filaments with the positive and negative projections are the same. These two types of filaments should be rather uniformly distributed over the lattice. In this case, it would occur that $M_z = 0$ in Eq. (4) and the magnetic cross section decreases to zero with the field decrease, and M_x in Eq. (4) decreases.

However, nothing of this kind is observed in the above experiment (Figs. 4 and 6b). This is related to the important circumstance that the magnetic field in the real situation is never directed exactly perpendicular to the axes of the filaments. When the field is approximately equal to the saturation field, a slight deviation of the magnetic field from the direction perpendicular to the axes of the filaments is sufficient for the projections of all filaments on their axis to take the same sign. With a further decrease in the external field H, the magnetization component parallel to the filament axis will increase and the demagnetizing field Eq. (6), which tends to equalize the N_+ and N_- numbers, will increase as well. The magnetic reversal of the filaments starts at the moment when the intensity and angle θ_h of the field $\mathbf{H} + \mathbf{H}_d$ are such that $|\mathbf{H} + \mathbf{H}_d| > H_f(\theta_h)$. At the magnetic reversal of a part of filaments, H_d decreases, θ_h increases, and $|\mathbf{H} + \mathbf{H}_d|$ decreases. The magnetic reversal of the filaments occurs till $|\mathbf{H} + \mathbf{H}_d|$ equals $H_f(\theta_h)$. Thus, the results of the neutron experiment can be described using Eqs. (4)–(6) by assuming a certain dependence $H_f(\theta_h)$ and the presence of a slight deviation (of several degrees) of the direction of the external field from the normal to the filament axes. As a result of these calculations, we succeeded at qualitatively reproducing the behavior of the magnetic scattering cross section shown in Figs. 4 and 6b. Note that the results are highly sensitive to the details of the behavior of $H_f(\theta_h)$. Based on these calculations, we can propose the following qualitative description of the observed behavior of the magnetic scattering cross section.

At the initial stage of the field decrease from the H_S value, only a small number of filaments experience the magnetic reversal and the cross section increases, since $I_H \propto (NM_s)^2 - 3M_x^2/4$ and M_x decreases with the

field decrease. The number of filaments that experienced the magnetic reversal starts to increase rather fast with the field decrease when the angle θ_h becomes on the order of $\pi/4$, i.e., when $H_d \approx 4\pi f M_s = 2fH_S$ becomes on the order of H (in our case, $f \approx 0.19$ and 0.13 in Fe/SiO_2 and Ni/Al_2O_3, respectively). When a large number of filaments experience the magnetic reversal, M_z in Eq. (4) strongly decreases and the cross section drops to zero at the further decrease in H. At $H = 0$, $N_+ \neq N_-$ (as indicated by the nonzero cross section), since the demagnetizing field does not exceed $H_f(0)$. When the negative field is applied, the cross section continues to somewhat decrease to the value $H \approx 2fH_S$. Again, this is related to the fact that the external field is not exactly perpendicular to the filaments. At the inverse course of the field, its component parallel to the axes of the filaments is directed to the same side as $\mathbf{H}_d$, which tends to equalize the N_+ and N_- numbers. At $H \geq 2fH_S$, no magnetic reversal of the filaments occurs and the cross section decreases smoothly.

5. CONCLUSIONS

To conclude, the unusual growth of the coherency of the array of magnetic nanofilaments during the magnetic reversal process for both positive and negative fields has been established. A theory was developed that qualitatively well describes the observed effects in the arrays of interacting ferromagnetic nanofilaments during magnetic reversal.

This work was supported by the Russian Foundation for Basic Research (project no. 10-02-00634-a).

REFERENCES

1. L. Sun, Y. Hao, C.-L. Chien, and P. C. Searson, IBM J. Res. Dev. **49**, 79 (2005).
2. K. S. Napolskii, A. V. Petukhov, A. A. Eliseev, et al., J. Appl. Crystallogr. **43**, 531 (2010).
3. E. A. Kelberg, S. V. Grigoriev, A. I. Okorokov, et al., Physica B **335**, 123 (2003).
4. H. Masuda and K. Fukuda, Science **268**, 1466 (1995).
5. I. V. Roslyakov, K. S. Napolskii, A. A. Eliseev, et al., Nanotechnol. Russia **4**, 176 (2009).
6. S. V. Grigoriev, N. A. Grigoryeva, and A. V. Syromyatnikov, JETP Lett. **85**, 449 (2007).
7. L. D. Landau and E. M. Lifshitz, *Course of Theoretical Physics*, Vol. 8: *Electrodynamics of Continuous Media* (Nauka, Moscow, 1982; Pergamon, New York, 1984).
8. S. V. Grigoriev, A. V. Syromyatnikov, A. P. Chumakov, et al., Phys. Rev. B **81**, 125405 (2010).
9. K. M. Lebecki, Mater. Sci. (Poland) **26**, 983 (2008).

Translated by L. Mosina